

Excess conductivity of overdoped $\text{Bi}_2\text{Sr}_2\text{CaCu}_2\text{O}_{8+x}$ crystals well above T_c

E. Silva

Dipartimento di Fisica "E. Amaldi" and Unità INFN, Università "Roma Tre," Via della Vasca Navale 84, 00146 Roma, Italy

S. Sarti, R. Fastampa, and M. Giura

Dipartimento di Fisica and Unità INFN, Università "La Sapienza," P. le Aldo Moro 2, 00185 Roma, Italy

(Received 20 December 2000; revised manuscript received 9 May 2001; published 19 September 2001)

We have used a multiterminal technique in order to measure the (a,b) plane excess conductivity $\Delta\sigma$ in several $\text{Bi}_2\text{Sr}_2\text{CaCu}_2\text{O}_{8+x}$ single crystals. We find that the experimental $\Delta\sigma$ does not follow a simple power law $\Delta\sigma \sim \epsilon^{-\alpha}$, with $\epsilon = \ln(T/T_c)$, and that it drops faster than the two-dimensional Aslamazov-Larkin law, $\alpha = 1$, with increasing temperature. In addition, data for samples with different doping do not scale on a universal curve. We discuss our data in terms of microscopic and Ginzburg-Landau theories, where high-momentum fluctuations are either not excited, or phenomenologically cut off. The experimental $\Delta\sigma$ drops even faster than the prediction of the extended microscopic theory. However, we can accurately describe all our data up to $T \approx 1.3 T_c$ with the GL theory, assuming a sample-dependent cutoff value. We relate the cutoff parameter to the doping level of our samples.

DOI: 10.1103/PhysRevB.64.144508

PACS number(s): 74.40.+k, 74.25.Fy, 74.72.Hs

I. INTRODUCTION

Since the discovery of high- T_c superconductors (HTCS's) the excess conductivity $\Delta\sigma$ due to superconducting fluctuations above T_c has been experimentally investigated.¹⁻¹⁶ While a general consensus exists on the extraordinary relevance of fluctuations in the determination of the superconducting properties in a wide range (several kelvins) around T_c , theoretical descriptions of the data have evolved in time, together with the availability of better-characterized samples, such as single crystals or crystalline-quality thin film. First interpretations were given using traditional models, such as the well-known Aslamazov-Larkin theory.¹⁷ In some cases, Maki-Thompson terms¹⁸⁻²⁰ were found necessary to fit the data,¹² while other experimenters found it unnecessary.^{1,7,13,15} Theoretical works proceeded to unveil other, previously neglected, contributions to the excess conductivity,²¹⁻²³ but unambiguous quantitative descriptions of the data are still lacking.

Among other interesting features, HTCS's present a pronounced anisotropy, even extreme in $\text{Bi}_2\text{Sr}_2\text{CaCu}_2\text{O}_{8+x}$ (BSCCO). This compound is of particular interest as a representative of a nearly two-dimensional superconductor, in the sense that the superconducting layers can be considered as almost decoupled. Only the divergence of the out-of-plane coherence length induces a crossover to a three-dimensional behavior,²⁴ but extremely close to T_c : the crossover region is estimated to be not wider than ~ 1 K. In fact, such crossover has been found below T_c (Ref. 25) from transport measurements in a magnetic field. Above T_c the crossover manifests itself in the excess conductivity by a change of slope:^{23,26-28} in the 3D region, very close to T_c , a 3D (Aslamazov-Larkin, AL)¹⁷ expressions holds, and

$$\Delta\sigma^{3D} = \frac{e^2}{32\hbar} \frac{1}{\xi_c(0) \epsilon^{1/2}} \quad (1)$$

while for temperatures even slightly above T_c a 2D AL formulation¹⁷ is appropriate:

$$\Delta\sigma^{2D} = \frac{e^2}{16\hbar d} \frac{1}{\epsilon}. \quad (2)$$

Here $\epsilon = \ln(T/T_c)$, e is the electron charge, d is the effective thickness of the superconducting layers and $\xi_c(0)$ is the zero-temperature out-of-plane correlation length. Similar dependencies have been sometimes observed,^{3,12,13,15,16} even if this is not a universal feature of the experiments.⁷ In fact, the observation of such a crossover is extremely sensitive to the choice of T_c , since it is expected to take place in the region $\epsilon \leq 0.01$, where small differences in the choice of T_c dramatically modify the ϵ dependence of $\Delta\sigma$.^{4,11} Moreover, in this temperature region sample inhomogeneities can affect the temperature dependence of $\Delta\sigma$,¹⁰ even if there are indications that such effect might be negligible in zero magnetic field.¹³

A second interesting and less studied region is the high-temperature range (up to $1.5 T_c$). In fact, it is well known that the original AL theory can be applied only close to the transition, while with increasing ϵ (e.g., above $\epsilon \sim 0.05$) it overestimates the weight of the fluctuations (technically, the low- q expansion of the fluctuation propagator and the q independence of the fermionic propagator employed in the original AL work¹⁷ are not valid approximations far from T_c , where the uniform mode is no longer the only relevant mode), giving rise to a $\Delta\sigma$ larger than it is actually measured. This statement is confirmed by several reports on both thin films and crystalline samples. In all the data on thin BSCCO films^{5,6,8,15} a 2D AL behavior is observed in some temperature region. However, the simple 2D AL description fails above ϵ values that are sample dependent, scattered from 0.05 (Ref. 5) up to 0.18 (Ref. 6). Interestingly, films from the same source present *different* extensions of the AL region.^{5,8,15} It is worth to stress that in some cases the range of validity for the AL expression resulted overestimated by

the incorrect definition of $\epsilon = T/T_c - 1$, instead of $\epsilon = \ln(T/T_c)$. As will be discussed in the following, the data on single crystals are often affected by the incorrect determination of the in-plane resistivity. There are then a very few, if any, reliable excess conductivity data in crystals. Mandal *et al.*³ employed a Montgomery analysis to extract the excess conductivity in one BSCCO crystal, and found a 2D AL range extending up to $\epsilon \approx 0.075$. Others^{2,7,9,13,16} took data with the simple four-probe configuration in BSCCO crystals, obtaining conflicting results. In general, data in BSCCO crystals were never compared to theories extended beyond the small ϵ region.

The extension of the AL result to higher temperatures for the case of a 2D, clean superconductor has been studied in Ref. 21: it has been shown that, taking into account the full q -vector dependence of the fermionic propagator, the excitation of high- q fluctuations is severely depressed with respect to the AL calculation. This has little consequences on the excess conductivity very close to T_c , where low- q modes are dominant, but strongly reduces $\Delta\sigma$ as far as T exceeds T_c . The excess conductivity results to be

$$\Delta\sigma = \frac{e^2}{16\hbar d} f_V(\epsilon), \quad (3)$$

where $f_V(\epsilon)$ has the limits $f_V = \epsilon^{-1}$ approaching T_c , and $f_V \sim \epsilon^{-3}$ for $T \gg T_c$. The function f_V does not contain parameters, so that Eq. (3) predicts a universal behavior for the two-dimensional excess conductivity (apart from the possible scaling factor d). First experimental investigations⁵ in BSCCO thin films agreed with Eq. (3) for $\epsilon < 0.1$. At high temperatures even Eq.(3) predicted a larger $\Delta\sigma$ than observed.^{5,15}

A second, very often used path that has been followed is the use of time-dependent Ginzburg-Landau theory (TDGL) to calculate the excess conductivity (paraconductivity). The usual TDGL theory in the Gaussian approximation is entirely equivalent²⁹ to the AL formulation at small ϵ , and Eqs. (1) and (2) are recovered. The paraconductivity as calculated in the TDGL-Gaussian approximation shares with the microscopic theory the same drawbacks in the q -dependence of the fluctuational spectrum. In order to overcome such limitations, it has been proposed long time ago to phenomenologically cutoff the fluctuational spectrum at a maximum wave vector, of order of the inverse correlation length.³⁰ Such approach found its roots in similar problems arising from the calculation of the excess diamagnetism,³¹⁻³³ where a cutoff was imposed on the energy spectrum of the excitations, instead. The cutoff approach was then used to extend the Gaussian approximation results for the paraconductivity to larger ϵ in three-dimensional amorphous superconductors,³⁰ in YBCO pellets³⁴ and films,^{4,11} and in textured BSCCO tapes.¹⁴ We are not aware of similar studies in HTCS single crystals.

It is clear that detailed, systematic analysis on BSCCO single crystals are desirable, in order to ascertain the nature of fluctuations far from T_c . However, the intrinsic, huge anisotropy of this compound poses severe constraints on the measurements of the true resistivity (ρ_{ab} , in-plane, and ρ_c ,

out-of-plane): while measurements in thin films performed in the common four-probe configuration give the correct values for ρ_{ab} , this is no longer true for measurements in crystals:³⁵⁻³⁸ the voltage drop in the four contacts, in-line configuration does not yield a quantity that is close to the in-plane resistivity, even approximately.^{37,38} This fact obscures some of the works performed in BSCCO crystals, and calls for appropriate treatment of the data. For similar reasons, analysis of the data for the excess conductance taken on noncrystalline materials, such as sintered pellets or thick tapes, can hardly give reliable, quantitative information.

Summarizing the indications given by the literature, it is possible to assert that the region $T_c \leq T \leq T_c + 1$ K is of very difficult experimental investigation, due to the reasons above mentioned. However, nontrivial dependences are clearly detectable in the excess conductivity above this temperature range. Moreover, this is the temperature range where 2D treatment should better apply to the excess conductivity in BSCCO. In addition, in a very few measurements in BSCCO crystals has been the resistivity correctly derived. Thus, the study of the high-temperature region in highly anisotropic BSCCO crystals is still far from being complete, and it is the main subject of this work.

In this paper, we present systematic measurements of the (a,b) plane excess conductivity in several, slightly overdoped, BSCCO single crystals. We show that an accurate determination of the in-plane resistivity ρ_{ab} is an unavoidable starting point for the study of the excess conductivity. Using a recently developed method,³⁸ based upon multiterminal measurements, we obtain ρ_{ab} measurements in crystals with the necessary accuracy. The data for the excess conductivity vs ϵ as measured in different samples do not scale together with a mere factor, especially far from T_c . We discuss the data in terms of existing theories for the fluctuational conductivity beyond the AL approach, comparing the findings of the microscopic²¹ and Ginzburg-Landau (GL) theories, where the role of high-momentum fluctuations is intrinsically depressed or phenomenologically cut off, respectively. We show that both approaches give identical results with an appropriate choice of the cutoff parameter in the GL theory. Our data, however, show a decrease of the excess conductivity which is faster than predicted by the microscopic theory, and depends on the doping of the sample in the high- ϵ region. Allowing the short-wavelength cutoff in the phenomenological theory to be a fitting parameter, we show that all our data can be fitted by the extended GL theory in the range $0.01 < \epsilon \leq 0.25$ (that is from $\sim T_c + 1$ K up to $\sim T_c + 25$ K). We find a correlation between the values of the cutoff and the doping level.

II. EXPERIMENTAL SECTION AND RESULTS

In anisotropic, bulk materials a single voltage measurement is not in general sufficient to obtain the resistivity.³⁸ The resistivity in BSCCO samples thicker than, e.g., $\sim 1 \mu\text{m}$, is related to the measured voltages by nontrivial relations. In particular, by means of multiterminal voltage measurements we have experimentally shown³⁸ that in typical BSCCO single crystals, usually a few tens of μm thick,

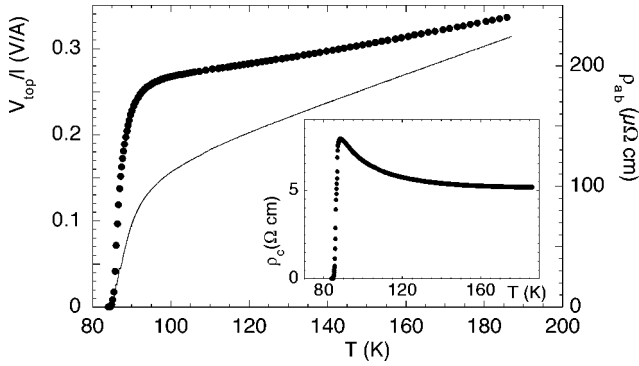


FIG. 1. In-plane voltage measurements in sample 11M, left scale, full circles, and extracted (see text) in-plane resistivity, right scale, continuous line. It is apparent that simple voltage measurements cannot be used as an evaluation of the behavior of the resistivity. To avoid crowding, only 30% of data is plotted. In the inset: the out of plane resistivity of the same sample.

none of the voltage measurements is proportional to the in-plane component of the resistivity, even in an approximate way. This statement becomes evident with the observation of Fig. 1, where it is shown how different the temperature dependence of the in-plane resistivity ρ_{ab} is and the in-plane voltage drop V_{top} (we employ here the accurate analysis developed in Ref. 38). It is evident that the assumption $V_{top} \sim \rho$ is incorrect, and can easily lead to wrong conclusions in the interpretation of the data. We remember that the extraction procedure depends on several geometrical parameters, which can hardly be controlled with high accuracy. This results in small uncertainties on the precise value of the resistivity, which, however, do not affect the following discussion. It is worth to stress that, using different sets of voltage measurements, the multiterminal technique allows for a quantitative determination of these uncertainties, while simple four probe measurements do not yield any estimate on the possible error related to the measurement method. Finally, the multiterminal measuring method allows for a simultaneous determination of the out of plane resistivity ρ_c , which can be used for a more complete characterization of the samples.

In this paper the resistivity is always obtained from multiterminal voltage measurements. On each sample, eight low resistance contacts were obtained by attaching with silver paste 25 μm gold wires onto freshly cleaved surfaces. Current was fed by a stepped current source (typical current intensity was $I=0.1$ mA) through one pair of the contacts, and voltage measured on the other three pairs by means of sensitive nanovoltmeters. Current was reversed for each datum point to cancel out thermal *emf*. Voltage measurements were taken in zero magnetic field from low temperature up to 270 K. Measurements upon cooling and warming gave no measurable differences. Screening the Earth's magnetic field with μ -metal sheets did not change the measured voltage in the temperature range of interest. We checked that all the measurements of relevance for this study were taken in the Ohmic regime.

We have performed a systematic study of the dc electrical transport properties on several high-quality BSCCO crystals.

TABLE I. Sample characteristics: critical temperatures, r ratio for the out-of plane resistivity (see text), cutoff parameters and effective fluctuating layer thickness (Ref. 48).

Sample	T_c (K)	r	K	d (\AA)
9M	86.2	0.66	0.63	4.0
11M	86.0	0.75	0.44	4.0
15M	86.6	0.74	0.50	3.8
16M	89.5	1.07	0.36	2.8
5M	86.6	0.85	0.41	3.0
7L	88.7	0.75	0.52	3.8

The crystals were grown using the directional solidification method.³⁹ Crystals of typical dimensions 1 mm \times 0.2 mm \times 0.01 mm were cleaved from the crystallites. Very smooth and shiny surfaces were observed under optical microscope. The samples were successively annealed in air for several hours to get a uniform oxygen concentration. According to the annealing procedure,⁴⁰ the crystals were slightly overdoped. To confirm this statement, we compared ρ_c of our samples to the values reported in Ref. 40. We used as parameter the ratio $r = (\rho_c^{\max} - \rho_c^{\min}) / \rho_c^{\min}$, where ρ_c^{\max} and ρ_c^{\min} are the maximum and the minimum value of ρ_c in the normal state. Using the data of Fig. 3 of Ref. 40, it turns out that r is a monotonically decreasing function of doping, with $r=1$ for optimally doped samples, $r \leq 1$ for overdoped samples, and $r > 1$ for underdoped samples. In our samples, $r \leq 1$, thus confirming that they are slightly overdoped. Experimental and fitting parameters (see below) are presented in Table I.

In Fig. 2 we present a typical in-plane resistive transition. An anomalous enhancement of the resistivity is observed in some of the crystals close to the zero-resistance temperature. We have observed the same anomaly also in BSCCO crystals from other sources. This feature is likely to be due to the breakdown of local conductivity,⁴¹ a fundamental assumption for the correct extraction of the resistivity.³⁸ The study of this

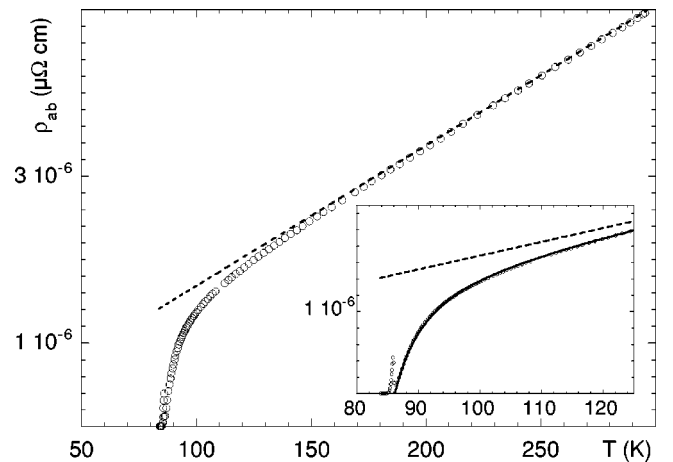


FIG. 2. Resistivity measurements in sample 9M. Open circles: experimental data, dashed straight line: normal state resistivity. Inset: enlarged view of the same data. Continuous line is the full resistivity: $\rho = (\rho_n^{-1} + \Delta\sigma)^{-1}$ with $\Delta\sigma$ calculated by the cutoff GL theory (see text). To avoid crowding, only 30% of data is plotted.

effect is under current investigation, and is out of the scope of this paper. The presence of this feature does not affect the present analysis of the data, since it lies in the temperature region below or very close to T_c . The transition temperatures (see below for the determination) are reported in Table I, and vary from 86.0 up to 89.5 K.

Once the data for the resistivity are obtained, a crucial step for the study of the excess conductivity is the determination of the normal state resistivity ρ_n . In fact, the in-plane excess conductivity is determined through the relation

$$\Delta\sigma = \frac{1}{\rho_{ab}(T)} - \frac{1}{\rho_n(T)}, \quad (4)$$

where $\rho_{ab}(T)$ is the measured resistivity. In all our samples, the resistivity is linear above ~ 160 K and always concave downward with decreasing T . We stress that this is not always true in the raw voltage data: in some of the crystals an upturn close to T_c appears. This is not due to sample quality, but only to the unavoidable mixing of ρ_{ab} and ρ_c in all voltage measurements.^{37,38} The extracted resistivity is *always* linear in T , with very low (or zero) residual resistivity extrapolated at zero temperature. We have chosen the normal state resistivity as the linear extrapolation at low temperatures, obtained from the fitting of the data above 160 K, as depicted in Fig. 2. This determination obviously prevents from an accurate extraction of the excess conductivity above ~ 140 K, where even small differences in ρ_n may determine large variations in $\Delta\sigma$. However, we have checked that below ~ 140 K the obtained $\Delta\sigma$ is robust against small changes in the choice of ρ_n , so that a wide range of temperatures can be analyzed with very small uncertainties. We remind that our crystals are overdoped, so that we do not expect a pseudo-gap opening that might affect the T dependence of ρ_n .

The final step is the determination of the critical temperature T_c . We here recall that in this paper our interest is focused in the temperature range above $\sim T_c + 1$ K, so that the determination of the critical temperature is not as crucial as in other studies,⁹ where the behavior in the close vicinity of T_c was the subject of interest.

The determination of T_c was accomplished as follows. We have calculated $\Delta\sigma$ and plotted $\Delta\sigma^{-1}$ vs T . Assuming the validity of Eq. (2) in a (even small) temperature range, by simple linear extrapolation we obtained T_c .¹¹ This procedure, graphically sketched in Fig. 3, was found to be self-consistent with the analysis performed in Sec. IV. The uncertainty of this procedure is well within the necessary accuracy for the purposes of this paper. Since we will mainly discuss data far from T_c , it is important to use the correct reduced temperature, $\epsilon = \ln(T/T_c)$.⁴²

In Fig. 4 we report the in-plane paraconductivity, $\Delta\sigma$, vs. the reduced temperature ϵ , in our samples and in the high temperature region. As can be seen, the data strongly bends downward with increasing ϵ : these results do not compare favorably to a simple AL framework. A different representation of the same data sheds light on a second aspect of our data: in Fig. 5 we report the data as normalized paraconductivity $\Delta\sigma/(e^2/16\hbar d)$ vs ϵ . Comparison with the 2D, AL law,

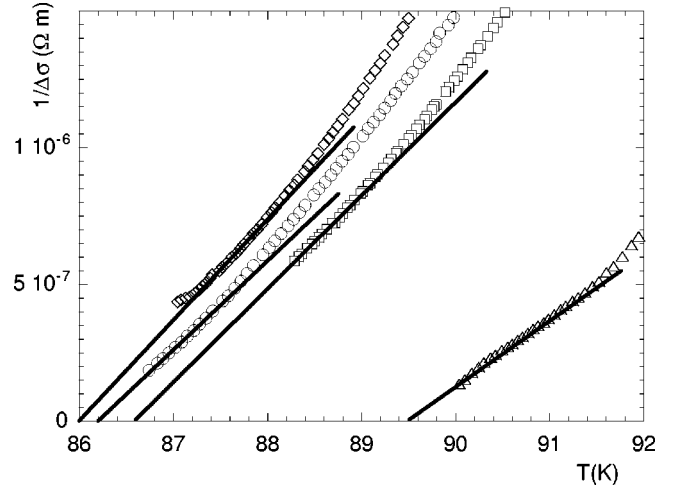


FIG. 3. Determination of T_c from the linear dependence of $\Delta\sigma^{-1}$ vs T in samples 9M (circles), 11M (diamonds), 15M (squares), and 16M (triangles). To avoid crowding, the data for the peak at T_c have been omitted and only 25% of data is shown.

Eq.(2), reveals that the pure 2D behavior (as indicated by a slope -1 in the $\ln \Delta\sigma$ vs $\ln \epsilon$ plot) is indeed observed, but in all samples it does not extend for more than 2 K above T_c (see also Fig. 3), since the tendency is to have an increasing slope with increasing temperature, that is a less pronounced excess conductivity. Interestingly, the latter feature shows up to a different extent in different samples. From the analysis of the data, it is then possible to assert that nonuniversal excess conductivity is observed at high ϵ . In the following we discuss our results in terms of microscopic and phenomenological theories for 2D excess conductivity.

III. THEORETICAL BACKGROUND

The extension of the calculation of the effects of superconducting fluctuations to the high-temperature region is

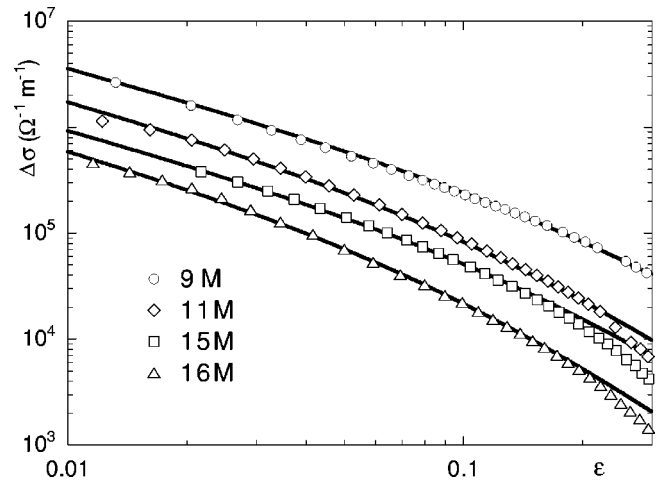


FIG. 4. $\Delta\sigma$ vs the reduced temperature ϵ for the same samples as in Fig. 3. The data are divided by a factor 2, 4, and 8 for samples 11M, 15M, and 16M, respectively, to avoid crowding. The continuous lines through the data are the fits with the 2D cutoffted GL expression, Eq. (9).

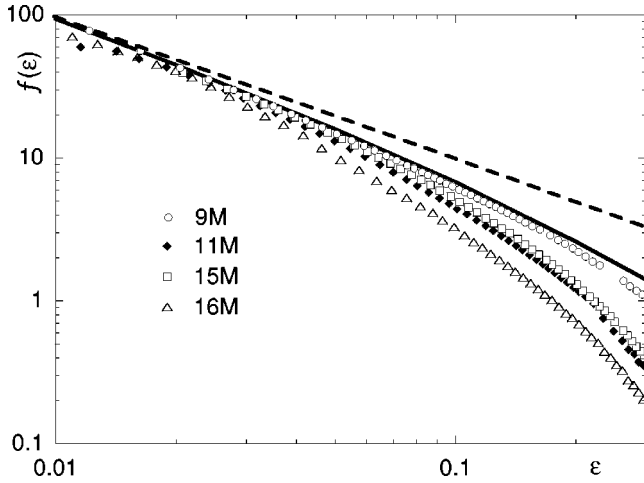


FIG. 5. High-temperature behavior of the normalized paraconductivity, $f = \Delta\sigma/(e^2/16\hbar d)$ vs the reduced temperature $\epsilon = \ln(T/T_c)$. Same samples as in Figs. 3 and 4. The differences at high ϵ are evident. The dashed straight line is the 2D AL law, Eq. (2), while the continuous line is the behavior of the extended microscopic calculation (Ref. 21) Eq. (3). As can be seen, already at low ϵ there is a significant departure from the AL prediction, and the full microscopic theory approximates the data only for small ϵ .

usually performed within two main general frames, namely, the phenomenological Ginzburg-Landau theory^{4,30,43} or through microscopic calculations.²¹ It is useful to briefly review the microscopic approach to the problem of the high-temperature limit of superconducting fluctuations.^{17,21,23} As discussed in the Introduction, apart from a small region around T_c the BSCCO system can be considered as almost 2D, so that we will restrict ourselves to the case of a 2D superconductor.

Within the microscopic approach, one uses the Kubo formula to relate the conductivity to the mean value of the correlator $[J, J]$. One then expands the latter in terms of Feynmann diagrams and considers the leading terms. It turns out¹⁷ that for $\omega \rightarrow 0$ the leading diagram is the Aslamazov-Larkin one (see Fig. 1 in Ref. 17). In the original work by Aslamazov and Larkin the diagram was calculated in the small ϵ and small q limit, and the result can be written as

$$\mathbf{j} = \mathbf{E}W \int C^2 \frac{q^3}{\{\epsilon + [\xi(0)q]^2\}^3} dq = \mathbf{E}W \int g_{AL}(q) dq, \quad (5)$$

where \mathbf{j} is the current density, \mathbf{E} is the applied field, W is a constant, $\xi(0)$ is the zero temperature correlation⁴⁴ length, Cq is the integral corresponding to the fermionic loops with $C \approx \text{const}$ in the limit of small q ,¹⁷ and the latter equality defines $g_{AL}(q)$. The small q approximation is valid close to T_c , since in that case the integrand decays very fast as a function of q . In the abovementioned limits, this result corresponds exactly to the conventional GL expression²⁹ (see also the Appendix).

This approximation loses its validity for large ϵ . To extend the calculation to higher temperatures, one has to take into account the full q dependence of both the fluctuational propagator and the fermionic loops. This has been done by

Reggiani *et al.* in the limit of a clean superconductor.²¹ The result of their calculation is that the function of q to be integrated in Eq. (5) can be written as, apart from a constant prefactor

$$g_V(q) = q^3 e^{-4\epsilon} \int_{-\infty}^{+\infty} \frac{1}{\sinh^2(2\pi y)} \frac{\text{Im} \tilde{\beta}(x, y, \epsilon)}{|\tilde{\beta}(x, y, \epsilon)|^4} \text{Im} \{ \tilde{\beta}(x, y, \epsilon) \times [\Sigma^*(x, y)]^2 \} dy, \quad (6)$$

where $\tilde{\beta}(x, y, \epsilon) = \psi(\frac{1}{2} + x + iy) - \psi(\frac{1}{2}) + \epsilon$, ψ is the digamma function, and

$$\Sigma^*(x, y) = \sum_n \frac{1}{\left[\left(n + \frac{1}{2} - iy \right)^2 + 1.173x \right]^{3/2}}, \quad (7)$$

where $x = \kappa [q\xi(0)]^2 e^{-2\epsilon}$, κ is a constant which depends on $\langle \mathbf{q} \cdot \mathbf{v} \rangle / |\mathbf{q}| |\mathbf{v}|$, and $\langle \rangle$ indicates the average over the Fermi surface ($\kappa = 0.203$ for a circular Fermi surface). Integrating Eq. (6) over q , one gets $\Delta\sigma$ as a function of ϵ , as reported as a thick line in Fig. 5. In the same figure, we report the experimental data for our samples. Two main differences between data and theory are evident: first of all, the experimental curves do not show an universal behavior, as it would be predicted from the theory. The second difference between data and theory is that the predicted $\Delta\sigma$ is always larger than the measured one. This is particularly evident for $\epsilon > 0.1$ and in most samples it is noticeable also for $\epsilon > 0.05$. This means that even the improved microscopic theory overestimates the extra conductivity at high ϵ , though the qualitative downward bending of the data is reproduced.

The discrepancies between the theory and the data should be found in the failure of some of the assumptions made in Ref. 21. In particular, the calculation was performed in the clean case: disorder and impurities are not considered. In addition, only the AL diagram was calculated, and a circular section of the Fermi surface was used. It has to be noted that all these conditions were somehow released in subsequent papers,²³ but the calculations were restricted, to our knowledge, to the small ϵ region.

The calculation of the extra conductivity at high ϵ from the microscopic theory goes beyond the scope of this paper. In the following, we will show the results that can be obtained by making use of a phenomenological GL approach to the problem. In particular, we will show that within this approach it is possible to describe all the experimental data with a single, sample-dependent parameter, whose physical meaning will be the subject of the last part of the paper. To better understand the main differences between the theory at low and high ϵ , we calculated $g_V(q)$ for several values of ϵ and compared it to the AL expression g_{AL} as defined in Eq. (5). In Fig. 6 we report the two expressions as a function of $q\xi(0)$, for $\epsilon = 0.1$. Similar or identical results are obtained for different values of ϵ . The two functions differ sensibly at high values of $q\xi(0)$, where g_V drops much faster than g_{AL} . Recalling that the AL approach finds an exact matching with the GL calculation, and guided by the shape of the microscopic $g_V(q)$, we inserted in the GL calculation a phenom-

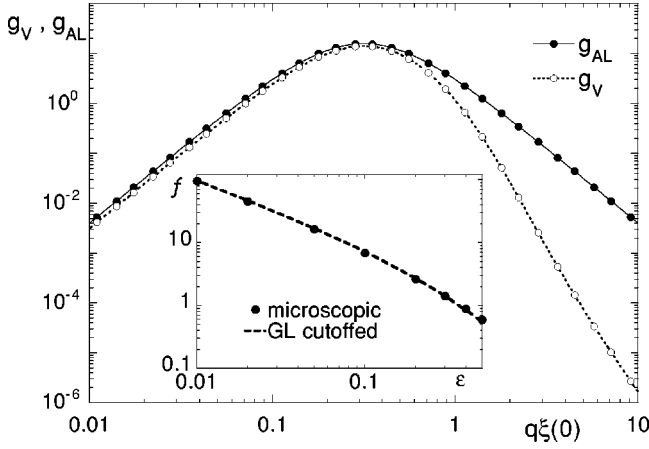


FIG. 6. Comparison of the Aslamazov-Larkin g_{AL} (full symbols) with the full microscopic calculation g_V (open symbols) for $\epsilon = 0.1$. g_V drops faster than g_{AL} at high $q\xi(0)$. In the inset, the comparison of $f(\epsilon)$ as obtained from the full microscopic theory (full dots) and from the GL cutoffted theory, Eq. (9), with $K=0.74$ (dashed line).

enological cutoff in the fluctuational spectrum. Similar calculations have been made by other authors,^{4,11,30,43} which introduced the cutoff in order to eliminate from the total conductivity the unphysical contributions arising from fluctuations whose size is less than the superconducting correlation length. Here we briefly summarize the main steps of the calculation, reported for completeness in the Appendix.

In the Ginzburg-Landau frame, one calculates the excess (fluctuation) conductivity by assuming that the total conductivity σ is the sum of the electrons and (fluctuating) pairs contributions. Interactions among normal electrons and fluctuations are taken into account only through the finite lifetime of the latter. To obtain the fluctuational contribution to σ one has to calculate the average of the current operator on the superconducting wave function, in which the momentum is shifted to take into account the presence of the applied electric field. For a two dimensional system (see the Appendix):

$$\langle J_x(t) \rangle = -\frac{\hbar e^*}{md} \int \frac{d^2 q}{(2\pi)^2} q_x C \left[\mathbf{k} = \mathbf{q} - \frac{e^*}{\hbar} \mathbf{A}(t); t \right], \quad (8)$$

where $C(\mathbf{q}, t)$ is the Fourier transform of the equal-time correlation function $C(\mathbf{r}, \mathbf{r}'; t, t) = \langle \psi(\mathbf{r}, t) \psi^*(\mathbf{r}', t) \rangle$. Performing the integration over the whole \mathbf{q} space, one gets the standard Gaussian correction to the normal state conductivity σ_n , which is equivalent to the AL result and, as discussed previously, is not accurate at high temperatures. The cutoff is introduced by limiting the integral over \mathbf{q} space to a square^{4,11} or a circle (see the Appendix). In the latter case, one obtains

$$\Delta\sigma(\epsilon) = \frac{e^2}{16\hbar d \epsilon} \frac{1}{(1 + \epsilon/K^2)^2}, \quad (9)$$

where $K = Q\xi(0)$ and Q is the radius of the circle in the \mathbf{q} space over which the integration is performed. Eq. (9) has

the correct limiting value for small ϵ , where it recovers the standard AL result $\Delta\sigma \propto \epsilon^{-1}$, and it drops much faster at higher temperatures. Further, the result of the cutoffted GL theory numerically reproduces the result of the improved microscopic theory if $K=0.74$ is chosen⁴⁴ (inset of Fig. 6).

IV. DISCUSSION

We obtain the excess conductivity $\Delta\sigma$ from the experimental data as described in Sec. II. The data for our samples are reported in Fig. 4. As explained, the reliable data range extends from 0.5–1 K above T_c up to $\sim T_c + 40$ K. The elaborations are then restricted to that temperature range. We also do not discuss the data for $\epsilon < 10^{-2}$, where the choice of T_c is the major issue. In the latter range, a 2D-3D crossover is predicted²⁸ and sometimes observed.^{3,13,16} Some of our data are compatible with this behavior, but for the reasons mentioned in Sec. II we do not discuss in detail this temperature region.

The first conclusion that can be drawn from the observation of the data is that even the extended microscopic theory²¹ does not describe correctly the strong decrease of $\Delta\sigma$ with increasing ϵ . This can be seen either in the normalized excess conductivity, Fig. 5, or in the absolute data, Fig. 4. In addition, the curves $\Delta\sigma(\epsilon)$ differ from sample to sample.

As discussed in the Introduction, this finding confirms previous results indicating that $\Delta\sigma$ does not have a single, universal behavior in BSCCO. The only feature that clearly emerges from the data is that a two-dimensional AL behavior is present, although in temperature ranges of various extension.

Coming back to the interpretation of the data, since the extended microscopic theory is not sufficient for a proper description of our data we resort to the phenomenological GL approach, extended in order to include a short-wavelength cutoff as described in Sec. III. The shape of the cutoffted GL expression, Eq. (9), depends only on the cutoff parameter K . In fact, the other parameter (the effective layer thickness d) is a mere scale factor, which absorbs all the uncertainties on the determination of the exact crystal thickness. However, values of the order of magnitude of the superconducting double CuO layers⁴⁵ ≈ 3.3 Å or of the inter-layer separation^{23,26} ≈ 15 Å are expected. The choice of the critical temperature T_c , which affects the shape of $\Delta\sigma$ in ~ 1 K range only, is not crucial for our purposes (the value of T_c has been fixed according to the procedure described in Sec. II).

In Fig. 4 we report some of the fits with Eq. (9) in different samples. As a general indication, we can safely state what follows.

(i) In all samples, Eq. (9) is a very good description of the data in the range $0.01 \leq \epsilon \leq 0.2$. This is a remarkable result, since this range roughly covers the temperature range ($T_c + 1$ K, $1.25T_c$).

(ii) The differences between the obtained values for K are much larger than the maximum estimated error (± 0.03), and they are relevant in the determination of the different shapes of $\Delta\sigma$ vs ϵ curves between different samples. This behavior

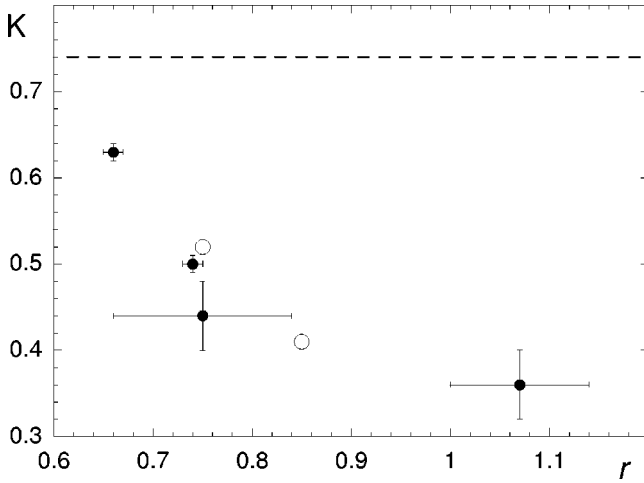


FIG. 7. The value of the cutoff K against the doping parameter $r = (\rho_c^{\max} - \rho_c^{\min}) / \rho_c^{\min}$ (r decreases with increasing doping, see text) in all the crystals investigated. The dashed line represents the equivalence with the microscopic theory. Error bars are different from sample to sample and reflect the uncertainty on the determination of both ρ_{ab} and ρ_c through the multiterminal analysis. Open symbols denote samples 5M and 7L, where it was not possible to estimate the error bars (Ref. 49).

is again a manifestation of the nonuniversal fluctuation conductivity.

(iii) The thickness of the effective superconducting layers, obtained through the fitting procedure is in the range $2.8 \text{ \AA} \leq d \leq 4 \text{ \AA}$, indicating that the double CuO planes act as independently fluctuating layers. This is in agreement with microwave results⁴⁶ and with temperature-dependent angular scaling properties of the magnetodissipation below T_c .⁴⁵

(iv) The values attained by the cutoff K vary in the range $0.36 < K < 0.63$. All these values are *below* the value 0.74, that would correspond to the extended microscopic theory (see Sec. III).

Keeping the original significance of the cutoff,³⁰ that is that fluctuations shorter than $\sim \xi(0)$ should be suppressed, we would get a cutoff of fluctuations of wavelengths shorter than $(1.5-3)\xi(0)$, which would be a reasonable number. However, within this frame, we cannot find some compelling argument neither for the sample variations of K , nor for the clear departure from the “expected” value 0.74.

In order to add information on this point, we have tried to correlate the K value with other features that can be obtained from the resistivity data. We did not observe a correlation between K and the normal state, in-plane resistivity, so that it appears that disorder does not play a fundamental role. We have then taken r as a parameter indicating the doping level (we recall that r is not a direct measure of the doping: instead, it is a monotonically decreasing function of it). In Fig. 7 we report the cutoff parameter K vs r . It is immediately clear that, even if according to the heat treatment⁴⁰ our doping level does not change much, a correlation clearly exists: with increasing doping, K increases. We now comment on this behavior and propose some speculation.

We first remind that pseudogap related phenomena are not expected, since our data are taken in the (slightly) overdoped

regime. In addition, we note that if such effects were present, we should get a $\Delta\sigma$ *larger* than the theoretical expectation, while we have the opposite result.

At the lowest level, we can identify K as a measure of the departure of $\Delta\sigma$ from the microscopic theory. From observation of Fig. 7 we then argue that our data tend to the microscopic prediction with increasing doping. Since the theory is developed for a conventional, clean superconductor with circular sections of the Fermi surface, we speculate that this departure might be a signature of a non circular section of the Fermi surface, which should evolve into a conventional metal for extreme overdoping. Interestingly, our data are compatible with an extrapolation to $K=0.74$ (i.e., applicability of the microscopic theory) for highly doped samples. While more work is needed in order to confirm this result, the indication is rather intriguing.

V. CONCLUSION

In conclusion, we have employed a multiterminal technique to measure the in-plane excess conductivity in several BSCCO crystals. We have shown that not too close to T_c no simple universal behavior appears. Our data are not described by the microscopic theory extended at high reduced temperature. However, all our data can be described by a phenomenological Ginzburg-Landau model for the dc fluctuational conductivity in a 2D superconductor, extended beyond the close vicinity of T_c by means of the introduction of a cutoff in the spectrum of the fluctuations. The agreement between our data and the GL model is excellent up to $T_c + 25$ K. The cutoff is found to be sample dependent. We found a correlation between the cutoff value and the doping level, suggesting that only extremely overdoped samples might be described by the conventional microscopic theory.

ACKNOWLEDGMENTS

We acknowledge fruitful discussions with R. Raimondi and D. Neri. We thank E. L. Wolf for supplying crystals and M. W. Coffey for careful reading of the manuscript. This work has been partially supported by INFM under PRA “HOP.”

APPENDIX: CALCULATION OF $\Delta\sigma$ WITH A SHORT-WAVELENGTH CUTOFF

We present here the explicit calculation of the 2D excess conductivity within the GL approach, with a phenomenological cutoff in the fluctuational spectrum. We model our system as a stack of uncorrelated layers, whose effective thickness is d (in the Lawrence-Doniach model this thickness corresponds to the interlayer separation; for a superconducting film, thin with respect to the correlation length, d is the film thickness). We assume the material to be isotropic in the (a,b) plane, neglecting the small in-plane anisotropy. We work in the Gaussian approximation, where the GL functional contains the order parameter ψ only up to the second order:

$$F = \int d\mathbf{r} \left[\sum_{j=x,y,z} \frac{\hbar^2}{2m_j} \left| \left(\frac{\partial}{\partial r_j} - \frac{ie^*}{\hbar} A_j \right) \psi(\mathbf{r}) \right|^2 + \alpha |\psi(\mathbf{r})|^2 \right], \quad (\text{A1})$$

where m_j are the effective masses, and $m_x = m_y = m$, $e^* = 2e$, $\alpha = a\epsilon$, $\epsilon = \ln(T/T_c)$ is the reduced temperature,⁴² the zero temperature in-plane correlation length is defined through $\xi(0) = \hbar/(2ma)^{1/2}$, and we have chosen the z axis to be perpendicular to the (a,b) planes. We are interested in the linear response in presence of an applied electric field along the (a,b) planes, e.g., along the x axis: $\mathbf{A} = (A, 0, 0)$. We then start from the standard time-dependent GL theory for a superconductor in presence of an external vector potential $\mathbf{A}(t) = -\mathbf{E}t$, where t is time (we use Système International units). The response function is given by the current operator averaged with respect to the noise, and it can be expressed as a function of the (Fourier transform of the) order parameter correlation function, $C(\mathbf{r}, t; \mathbf{r}', t') = \langle \psi(\mathbf{r}, t) \psi^*(\mathbf{r}', t') \rangle$. The equal time response reads

$$\langle J_x(t) \rangle = -\frac{\hbar e^*}{md} \int \frac{d^2q}{(2\pi)^2} q_x C \left[\mathbf{k} = \mathbf{q} - \frac{e^*}{\hbar} \mathbf{A}(t); t, t \right], \quad (\text{A2})$$

where the momentum dependence has been shifted from \mathbf{k} to the new vector $\mathbf{q} = \mathbf{k} + (e^*/\hbar)\mathbf{A}(t)$, and in a nearly two-dimensional superconductor $d^3q/(2\pi)^3 \rightarrow (1/d) \times [d^2q/(2\pi)^2]$ in the integration. In the frame of the linear response, the quadratic terms in the vector potential can be neglected, and for the equal time correlator [see, e.g., Eq. (4) of Ref. 47 for an explicit expression of $C(\mathbf{q}; t, t)$] we finally get

$$C(\mathbf{q}; t, t) = 2k_B T \Gamma_0 \int_0^{+\infty} ds \exp \left(-2\Gamma_0 \alpha s - \Gamma_0 \hbar^2 s \frac{(q_x^2 + q_y^2)}{m} - \frac{\Gamma_0 \hbar e^*}{m} E q_x s^2 \right), \quad (\text{A3})$$

where the relaxation time $\Gamma_0 = (8k_B T / \hbar \pi a)$ is evaluated from the microscopic theory.¹⁹ Calculation of Eq. (A2) is

now possible in polar coordinates, and after some manipulation we get

$$\langle J_x \rangle = -\frac{k_B T \hbar e^* \Gamma_0}{\pi m d} \int_0^{+\infty} ds e^{-2\Gamma_0 \alpha s} \times \int_0^Q dq q^2 e^{-(\Gamma_0 \hbar^2 / m) s q^2} I_1 \left(-\frac{e^* E \Gamma_0 \hbar}{m} q s^2 \right), \quad (\text{A4})$$

where on the integration on q we have explicitly put a cutoff on the modulus of the fluctuation wave vector (we used a similar approach⁴⁶ for the calculation of the microwave excess conductivity). The cutoff simulates in the GL frame the effect of the reduced importance of high-wave vector fluctuations which, in the microscopic theory, comes from the q dependence of the normal electrons propagator. We incidentally point out that letting $Q \rightarrow \infty$ one recovers exactly the Gaussian result for a thin film.^{17,19}

In the frame of the linear response, one can expand the Bessel function $I_1(x)$ for small arguments. Performing the integral over s in Eq. (A4), one then gets

$$\langle J_x \rangle = \frac{e^{*2} E}{16d\hbar} \int_0^Q \left[\frac{q\xi(0)}{\epsilon + [q\xi(0)]^2} \right]^3 d[q\xi(0)] \quad (\text{A5})$$

which, in the limit $Q \rightarrow \infty$ is equivalent to the AL result, Eq. (5). Integration over $q\xi(0)$ is trivial, and one finally gets the excess conductivity, defined through $\langle J_x \rangle = \Delta \sigma E$, with

$$\Delta \sigma(\epsilon) = \frac{e^2}{16\hbar d \epsilon} \frac{1}{(1 + \epsilon/K)^2}, \quad (\text{A6})$$

where $K = Q\xi(0)$ is an adimensional cutoff which has to be determined by the experiments (the cutoff value is here numerically different by a factor $\sqrt{2}$ from the one defined in Ref. 4, due to the different integration domain). This cutoff is the single parameter introduced in the modified expression for $\Delta \sigma$ (we mention that previous calculations using the Kubo formula⁴³ introduced two different cutoffs along x and y , respectively).

¹M. Ausloos and Ch. Laurent, Phys. Rev. B **37**, 611 (1988).

²J. J. Wnuk, L. W. M. Schreurs, P. J. T. Eggenkamp, and P. J. E. M. van der Linden, Physica B **165-166**, 1371 (1990).

³P. Mandal, A. Poddar, A. N. Das, B. Ghosh, and P. Choudhury, Physica C **169**, 43 (1990).

⁴R. Hopfgartner, B. Hensel, and G. Saemann-Ischenko, Phys. Rev. B **44**, 741 (1991).

⁵G. Balestrino, M. Marinelli, and E. Milani, Phys. Rev. B **46**, 14 919 (1992).

⁶S. Labdi, S. Megtert, and H. Raffy, Solid State Commun. **85**, 491 (1993).

⁷M. O. Mun, S. I. Lee, S. H. Suck Salk, H. J. Shin, and M. K. Joo, Phys. Rev. B **48**, 6703 (1993).

⁸V. Calzona, M. R. Cimberle, C. Ferdeghini, G. Grasso, D. V. Livanov, D. Marré, M. Putti, A. S. Siri, G. Balestrino, and E. Milani, Solid State Commun. **87**, 397 (1993).

⁹A. K. Pradhan, S. B. Roy, P. Chaddah, C. Chen, and B. M. Wanklyn, Phys. Rev. B **50**, 7180 (1994).

¹⁰W. Lang, Physica C **226**, 267 (1994).

¹¹A. Gauzzi and D. Pavuna, Phys. Rev. B **51**, 15 420 (1995).

¹²W. Holm, Ö. Rapp, C. N. L. Johnson, and U. Helmerson, Phys. Rev. B **52**, 3748 (1995).

- ¹³A. Pomar, M. V. Ramallo, J. Mosqueira, C. Torron, and F. Vidal, *Phys. Rev. B* **54**, 7470 (1996).
- ¹⁴Q. Wang, G. A. Saunders, H. J. Liu, M. S. Acres, and D. P. Almond, *Phys. Rev. B* **55**, 8529 (1997).
- ¹⁵M. R. Cimberle, C. Federghini, E. Giannini, D. Marré, M. Putti, A. Siri, F. Federici, and A. Varlamov, *Phys. Rev. B* **55**, R14 745 (1997).
- ¹⁶S. H. Han, Yu. Eltsev, and Ö. Rapp, *Phys. Rev. B* **57**, 7510 (1998).
- ¹⁷L. G. Aslamazov and A. I. Larkin, *Fiz. Tverd. Tela (Leningrad)* **10**, 1104 (1968) [*Sov. Phys. Solid State* **10**, 875 (1968)]; *Phys. Lett.* **26A**, 238 (1968).
- ¹⁸K. Maki, *Prog. Theor. Phys.* **39**, 897 (1968); **40**, 193 (1968).
- ¹⁹W. J. Skocpol and M. Tinkham, *Rep. Prog. Phys.* **38**, 1049 (1975).
- ²⁰K. Maki and M. Thompson, *Phys. Rev. B* **39**, 2767 (1989).
- ²¹L. Reggiani, R. Vaglio, and A. A. Varlamov, *Phys. Rev. B* **44**, 9541 (1991).
- ²²V. V. Dorin, R. A. Klemm, A. A. Varlamov, A. I. Buzdin, and D. V. Livanov, *Phys. Rev. B* **48**, 12 951 (1993).
- ²³A. A. Varlamov, G. Balestrino, E. Milani, and D. V. Livanov, *Adv. Phys.* **48**, 655 (1999).
- ²⁴W. E. Lawrence and S. Doniach, in *Proceedings of the 12th International Conference on Low Temperature Physics*, edited by E. Kanda (Kiegaku, Tokio, 1971), pp. 361-362.
- ²⁵R. Fastampa, M. Giura, R. Marcon, and E. Silva, *Phys. Rev. Lett.* **67**, 1795 (1991); R. Marcon, E. Silva, R. Fastampa, and M. Giura, *Phys. Rev. B* **46**, 3612 (1992).
- ²⁶R. A. Klemm, *J. Low Temp. Phys.* **16**, 381 (1974).
- ²⁷K. Yamaji, *Phys. Lett.* **38A**, 43 (1972).
- ²⁸L. N. Bulaevskii, *Int. J. Mod. Phys. B* **4**, 1849 (1990).
- ²⁹E. Abrahams and J. W. F. Woo, *Phys. Lett.* **27A**, 117 (1968).
- ³⁰W. L. Johnson, C. C. Tsuei, and P. Chaudhari, *Phys. Rev. B* **17**, 2884 (1978).
- ³¹B. R. Patton, V. Ambegaokar, and J. Wilkins, *Solid State Commun.* **7**, 1287 (1969).
- ³²J. Kurkijarvi, V. Ambegaokar, and G. Eilemberger, *Phys. Rev. B* **5**, 868 (1972).
- ³³J. P. Gollub, M. R. Beasley, R. Callarotti, and M. Tinkham, *Phys. Rev. B* **7**, 3039 (1973).
- ³⁴P. P. Freitas, C. C. Tsuei, and T. S. Plaskett, *Phys. Rev. B* **36**, 833 (1987).
- ³⁵R. Busch, G. Ries, H. Werthner, G. Kreiselmeyer, and G. Saemann-Ischenko, *Phys. Rev. Lett.* **69**, 522 (1992).
- ³⁶Y. M. Wan, T. R. Lemberger, S. E. Hebboul, and J. C. Garland, *Phys. Rev. B* **54**, 3602 (1996).
- ³⁷G. A. Levin, *J. Appl. Phys.* **81**, 714 (1997).
- ³⁸M. Esposito, L. Muzzi, S. Sarti, R. Fastampa, and E. Silva, *J. Appl. Phys.* **88**, 2724 (2000).
- ³⁹H. J. Tao, A. Chang, F. Lu, and E. L. Wolf, *Phys. Rev. B* **45**, 10 622 (1993).
- ⁴⁰T. Watanabe, T. Fujii, and A. Matsuda, *Phys. Rev. Lett.* **79**, 2113 (1997).
- ⁴¹S. Sarti, M. Esposito, R. Fastampa, M. Giura, and E. Silva, *Physica C* **332**, 225 (2000).
- ⁴²L. P. Gor'kov, *Zh. Éksp. Teor. Fiz.* **36**, 1918 (1959) [*Sov. Phys. JETP* **9**, 1364 (1959)].
- ⁴³A. Gauzzi, *Europhys. Lett.* **21**, 207 (1993).
- ⁴⁴For the sake of compactness, throughout the paper we use only the GL zero-temperature correlation length $\xi(0)$ instead of the microscopic coherence length $\xi_0 = \xi(0)/0.74$, formally more appropriate in the discussion of the microscopic theories. As a consequence, in Sec. III and in the Appendix the cutoff $K = 0.74$ means a momentum cutoff $Q = \xi_0^{-1}$.
- ⁴⁵E. Silva, S. Sarti, M. Giura, R. Fastampa, and R. Marcon, *Phys. Rev. B* **55**, 11 115 (1997).
- ⁴⁶D. Neri, R. Marcon, E. Silva, R. Fastampa, L. Iacobucci, and S. Sarti, *Int. J. Mod. Phys. B* **13**, 1097 (1999); D. Neri, R. Fastampa, M. Giura, R. Marcon, S. Sarti, and E. Silva, *J. Low Temp. Phys.* **117**, 1099 (1999).
- ⁴⁷D. Neri, E. Silva, S. Sarti, R. Marcon, M. Giura, R. Fastampa, and N. Sparvieri, *Phys. Rev. B* **58**, 14 581 (1998).
- ⁴⁸The thickness d has been chosen as to give $f(\epsilon) = 1/\epsilon$ in the limit of small ϵ .
- ⁴⁹In all samples but 5M and 7L several voltages were available, so it was checked that the extraction of the excess conductivity was not dependent on the pair of voltages chosen. In samples 5M and 7L only three voltage curves were available, so this cross check could not be performed.